

Development and validation of atmospheric gene flow model for assessing environmental risks from transgenic corn crops

Junming Wang¹, Xiusheng Yang²

(1. Department of Agricultural Sciences, Tennessee State University, Nashville, TN 37209, USA;

2. Department of Natural Resources Management and Engineering, University of Connecticut, Storrs, CT 06268-4087, USA)

Abstract: Pollen-mediated gene flow from genetically modified plants to non-target plants is a concern of crop growers, seed companies, the general public, and the scientific communities. Although there have been descriptive and mechanistic models to describe pollen dispersion, there has rarely been a comprehensive mechanistic model to dynamically simulate pollen release, dispersion, and deposition and to finally relate them to the gene flow (outcrossing). This research developed and validated such a comprehensive mechanistic model for corn crop gene flow risk management. Dynamic pollen dispersion and deposition were predicted by a 3-D random walk model according to inputs of weather data and plant and domain characteristics. Actual gene flow (outcrossing ratio) was obtained according to predicted grand total deposition flux at silk height during the whole pollination season. The model was validated by experimental data and was appropriate to predict gene flow with acceptable accuracy under different atmospheric and environmental conditions; on average, the ratios of measured and simulated values ranged from 0.82 to 1.21, while R^2 ranged from 0.56 to 0.68. The model can be easily adapted for other genetically modified crops.

Keywords: corn, pollen, gene flow, model, simulation, random walk

DOI: 10.3965/j.issn.1934-6344.2010.02.018-030

Citation: Junming Wang, Xiusheng Yang. Development and validation of atmospheric gene flow model for assessing environmental risks from transgenic corn crops. *Int J Agric & Biol Eng*, 2010; 3(2): 18–30.

1 Introduction

The large-scale commercial release of genetically modified crops (GMCs) may pose serious environmental risks^[1,2]. Pollen dispersion from GMCs can transfer the “super genes” to non-domesticated relatives, and create “superweeds” to non-target crops, causing genetic pollution. Many gene flow experiments have been conducted for corn crops, started as early as 1940s^[3-9]. However, significant differences among different experiments existed, and these differences were mainly

caused by conditions of source production, size of the source area, and weather (mostly wind speed and atmospheric stability)^[10]. Comprehensive field studies on gene flow under different conditions of GMCs field size, source production, wind speed, and atmospheric stability are costly and not practical. Therefore, development and application of models in gene flow studies are required.

Various descriptive models have been used to depict pollen dispersion in the horizontal or vertical plane^[10-15]. However, these models were limited by their descriptive nature^[16]. Such descriptive models do not have the power to analyze the effects of the controlling factors, should not be extrapolated outside the observation range, and cannot be used to simulate or predict the dynamics of the dispersion process.

Studies on atmospheric transport have shown that scalar dispersion is heavily dependent on turbulence and atmospheric stability^[17]. Some mechanistic models of

Received date: 2010-03-10 **Accepted date:** 2010-05-20

Biography: Junming Wang, Ph.D., assistant professor, majored in plant and environmental science. Department of Agricultural Sciences, Tennessee State University, Nashville, TN 37209, USA. Email: wangjunming@hotmail.com

Corresponding author: Xiusheng Yang, Ph.D., Professor, Department of Natural Resources Management and Engineering, University of Connecticut, Storrs, CT 06269-4087, USA. Phone: (860) 486-0135, Fax: (860) 486-5408, Email: xiusheng.yang@uconn.edu

atmospheric transport are quite well developed for simulating transport processes in and above vegetation canopies^[18-23]. A background assumption in these transport models is that the movement of a scalar in the atmosphere is controlled by turbulent atmospheric flow, settling and diffusion of the particles, and uptake by the intercepting elements. Examples of successful applications of mechanistic models to pollen transfer were Okubo and Levin^[24], Tufto et al.^[25], Klein et al.^[26], and Aylor et al.^[27].

Most dispersion models can be broadly classified as Lagrangian or Eulerian based on the type of reference frame used for formulation^[28]. The application of Eulerian models for estimating scalar transfer by turbulence within and above plant canopies has been limited by the inability to properly treat the dispersion of material from nearby sources. Lagrangian models do not suffer from this deficiency since they consider the diffusion of materials from both nearby and far away sources explicitly^[29]. One example of the Lagrangian models to simulate particle trajectories in three dimensions is Wilson and Shum^[30], which did not include particle transport in canopy.

Although much has been learned about pollen dispersion and gene flow in model development, currently lacking in the literature is a comprehensive simulation system to simulate pollen dynamic release, dispersion, and deposition and relate them to the final outcrossing. The objective of this study was to develop and validate such a simulation model for transgenic corn crops.

2 Modeling theory

A computer-run simulation model was developed in this study to predict the gene flow from transgenic corn plants to their relatives. The model consisted of four major components (submodels): source strength, pollen dispersion, deposition, and fertilization. The overall structure of the model is depicted in Figure 1.

By taking field dimension and weather data as inputs, the model predicts the dynamic pollen release, three-dimensional pollen concentrations and depositions, and the final two-dimensional outcrossing ratios in the receptor field. The theoretical considerations of the

model are described as follows.

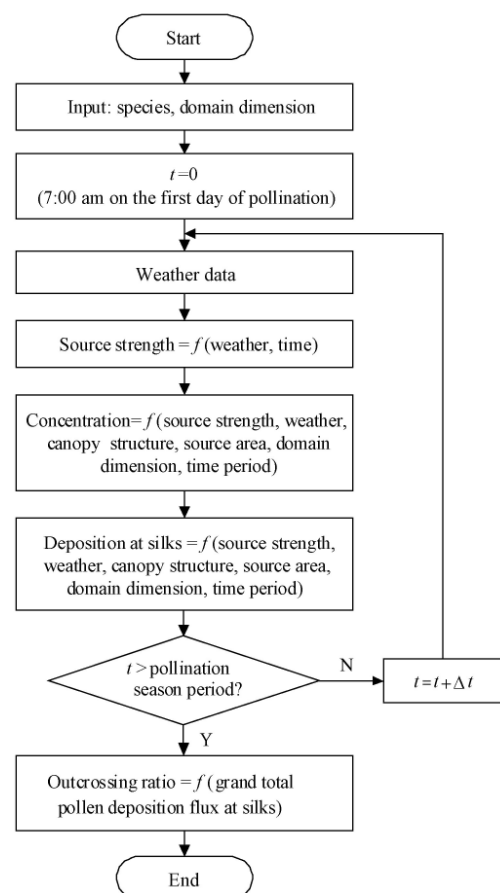


Figure 1 Flowchart of the overall model

2.1 Source strength

The source strength $Q_0(t)$ (grains/m²/s) is predicted according to time (t) and weather condition (precipitation) by the empirical data obtained in this study (See section 4.1 Experiments; see Table 1 for the symbol notations). If there is no precipitation, the source strength uses the measured data at the corresponding pollination time. Otherwise, the source strength is set to 0.

2.2 Wind calculation

The Obukhov Length (L), friction velocity (U), wind direction, and plant height were used to calculate the 3-D wind statistics field (mean wind speed with height) following Aylor and Flesch^[20]. If two adjacent field areas have plants of different heights, the wind fields in the areas are different. Even in the same area, the wind may have some transition when it comes from the edge extending to the downwind side. The equations for the transition wind calculations are based on Flesch and Aylor^[31].

Table 1 Symbols used in the model

Symbol	Unit	Meaning
$c(x, y, z, \Delta t)$	grains/m ³ /s	Concentration at a certain point (x, y, z) and during time period t
$DS(x, y, z, \Delta t)$	grains/m ² /s	Deposition flux density during t
d	m	Zero plane displacement distance
dA_{nm}	m ²	Subsector area in source
dt	s	Time step of one flight
dx	m	Displacement on x axis during dt
dy	m	Displacement on y axis during dt
dz	m	Displacement on z axis during dt
E^x	Unitless	Efficiency for horizontal deposition
E^z	Unitless	Efficiency for vertical deposition
f_x	Unitless	Horizontal fraction of leaf area density
f_z	Unitless	Vertical fraction of leaf area density
GTD	grains/m ²	Grand total deposition flux
$G(z, u, v, w)$	s ⁻¹	Rate of deposition at height z with certain turbulent velocities
g	m/s ²	Acceleration of gravity
h	m	Height of plant
h_m	m	Measurement height of wind data
k	Unitless	Karman constant (0.4)
L	m	Obukhov Length
L_{vi}	m	Characteristic leaf dimension
l_s	m	detection surface length
m	Unitless	Radially segmented number on source radius
Np	Grains	Released pollen grain number from each subsector
n	Unitless	Angularly sector number in source
OSN	kernel/m ²	Outcrossed seed number
$OutR$	Unitless	Outcrossing ratio
PF	Unitless	Probability of a pollen grain deposited
P_G	Unitless	Fraction of a grain deposited that reaches ground
Q_0	grains/m ² /s	Source strength
q_u	Unitless	Parameter for alongwind turbulence calculation
q_v	Unitless	Parameter for crosswind turbulence calculation
q_w	Unitless	Parameter for vertical turbulence calculation
r	m	Source, buffer, or receptor radius
r_c	m	Detection cylinder radius
TDF	grains/m ²	Total deposition flux during 2-hr pollen viable period
t	s	Time
u^*	m/s	Friction velocity
$\bar{u}(z)$	m/s	Mean horizontal wind velocity at height of z
u	m/s	Alongwind turbulent velocity
v	m/s	Crosswind turbulent velocity
v_s	m/s	Settling velocity of the pollen
w	m/s	Vertical turbulent velocity
w_s	m	Detection surface width
Z	Unitless	Uniform distribution random number
z	m	Height
z^{old}	m	Height of the grain at the previous time step
δt	S	Pollen residence time
θ	degree	Polar coordinate angle of a point
θ_1	degree	Polar coordinate angle of wind vector
θ_2	degree	Inputted mean wind direction
ρ	m	Polar coordinate radius

σ_u	m/s	Standard deviation of wind velocity in mean wind direction
σ_v	m/s	Standard deviation of wind velocity in crosswind direction
σ_w	m/s	Standard deviation of vertical wind velocity
Δt	s	Each simulation time period (900)
ΔV	m ³	Detection cylinder volume
Δz_c	m	Detection cylinder height

2.3 Pollen dispersion

The pollen dispersion sub-model is based on the random walk theory^[30]. The flowchart is shown in Figure 2. The random flight of each pollen particle is simulated in a sequence of short time steps, during each of which the particle moves by

$$dx = [\bar{u}(z) + u]dt, \quad dy = vdt, \quad dz = (w - v_s)dt \quad (1)$$

Where: $u(z)$ is the mean along wind velocity at the present height of the particle; u , v , and w are the along wind, crosswind, and vertical turbulent velocities, respectively; and v_s is the settling velocity of the particle^[32]. The velocity fluctuations can be formulated as^[31].

$$u = q_u \sigma_u, \quad v = q_v \sigma_v, \quad w = q_w \sigma_w \quad (2)$$

Where: q_u , q_v , and q_w are unitless parameters obtained in a form of Markov chain. The detailed description can be found in Wilson and Shum^[31].

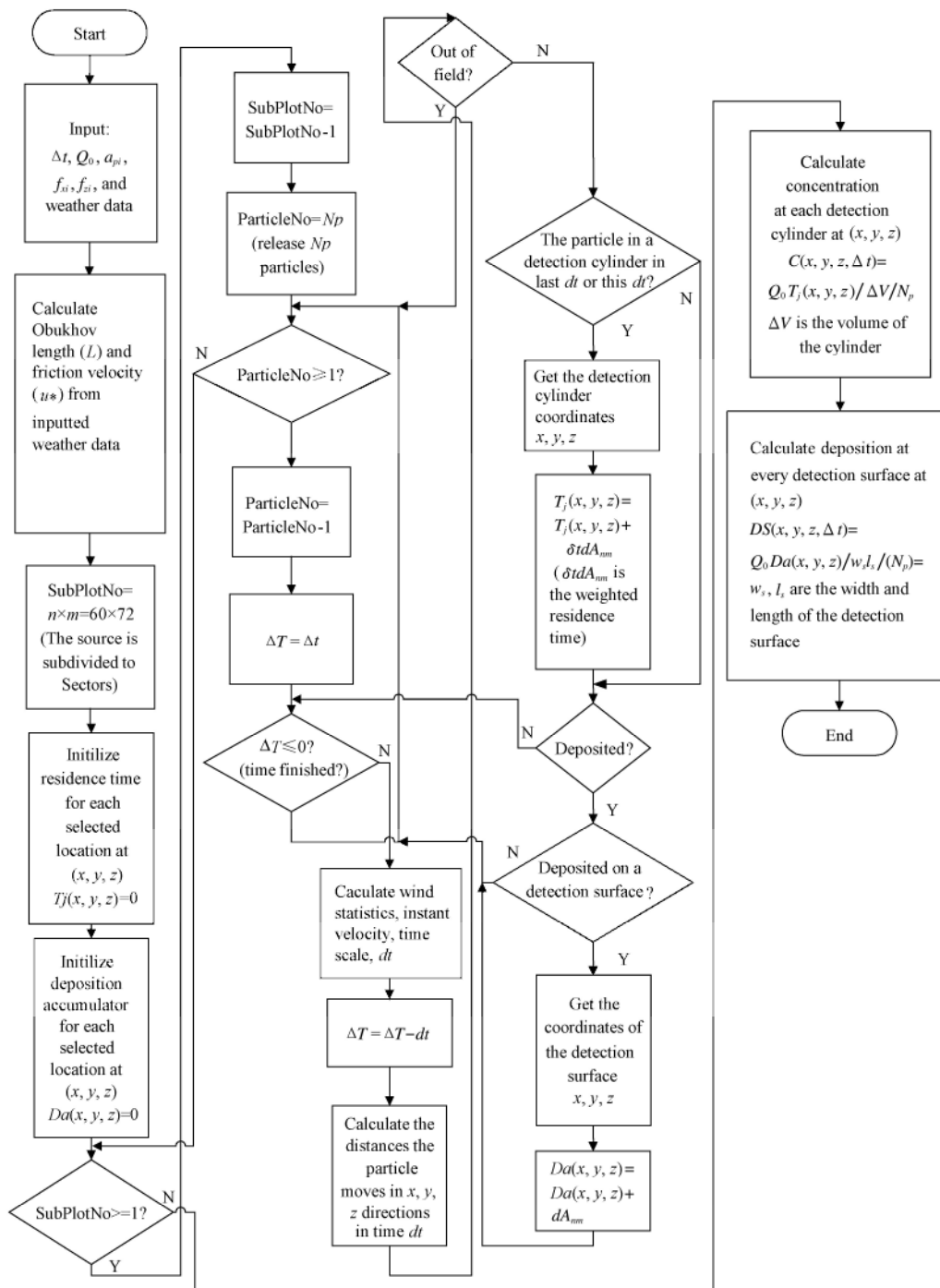
The source (circular area) was divided radially ($n = 60$) and angularly (by $m = 72$) into sectors of area dA_{nm} . For a given number of pollen grains (Np) released sequentially and independently from each sector, the model tracks each particle until it deposits on plants or ground, flies out of the simulation domain, or runs out of the simulation time. The n and m numbers are determined by computer computation power, and output grid resolution. The larger the numbers, the slower the computer speed. Using a 2.5 GHz duo core PC computer with 2 GB memory, the model runs two minutes to complete each 15 min simulation period. The sector arc and radial length should be at least 3 times less than the output grid length to guarantee the released particles to pass through each grid.

For predicting the concentration $c(x, y, z, \Delta t)$ at a certain point (x, y, z) during time period Δt , the “detection cylinder” is defined with radius r_c and depth Δz_c centered

on z and volume $\Delta V = \pi r_c^2 \Delta z_c$. Each time a particle from sector nm spends time δt within a detection cylinder at position (x, y, z) , a weighted residence time accumulator $T_j(x, y, z)$ is incremented by δtdA_{nm} . Mean

concentration $c(x, y, z, \Delta t)$ during simulation time period Δt is calculated, after all particles from all source sectors have flown, as

$$c(x, y, z, \Delta t) = Q_0 T_j(x, y, z) / \Delta V N_p \tag{3}$$



Note: a_{pi} , f_{xi} , and f_{zi} are plant characteristics defined in Table 2 (see Table 1 for symbol notations)

Figure 2 Flowchart of the pollen dispersion and deposition submodels

2.4 Pollen deposition

2.4.1 Pollen deposition on plants

Following Aylor and Ferrandino^[19] and Aylor and Flesch^[20], pollen grain deposition on or interception by

plants is determined by the probability that a pollen grain is deposited or intercepted during a time step (Figure 2). The probability of a pollen grain being deposited on or intercepted by the corn plants during each time step (PF)

is defined in terms of the rate of deposition $G(z, u, v, w)$ [s^{-1}], such that $PF=G \cdot dt$. The rate of deposition G depends on the area densities of the intercepting elements and the velocities u, v, w [20], as

$$G = (v_s - w) \cdot f_x a_p E^x dt + \sqrt{(\bar{u} + u)^2 + v^2} \cdot f_z \cdot a_p E^z dt \tag{4}$$

Where: E^x and E^z are the efficiencies for horizontal and vertical deposition. While E^x is assumed to be 1 [20], E^z is defined by

$$E^z = \frac{0.86}{1 + 0.442 \left(\sqrt{(\bar{u} + u)^2 + v^2} \tau_R / L_{vi} \right)^{-1.967}} \tag{5}$$

Where: t_R is the particle relaxation time. $\tau_R = v_s / g$, where g is the acceleration of gravity.

The variables of a_{pi} , f_{xi} , and f_{zi} are plant characteristics defined in Table 2.

Table 2 Required domain and plant input parameters

Symbol	Unit	Meaning
r_i	m	Field radius
h_i	m	Plant height
a_{pi}	m^2/m^3	Leaf area density as a function of height
f_{xi}, f_{zi}	Unitless	Horizontal and vertical fractions of a_{pi} as a function of height
L_{vi}	m	Characteristic leaf dimensions

For each line-of-flight segment of a trajectory, a random number Z is chosen from a uniform distribution between 0 and 1. If Z is less than PF , the pollen is deposited on the plants [19]. Otherwise, the pollen continues to fly based on Equation (1).

For calculating deposition flux density during the simulation time period $\Delta t(s)$, the “horizontal detection surface” will be located at a location (x, y, z) where the deposition flux density is needed to be predicted. The “detection surface” is defined by a rectangular area with width w_s and a length l_s . Each time a pollen grain from sector nm is deposited on it, the deposition accumulator $Da(x, y, z)$ will be added by dA_{nm} . The deposition flux density, $DS(x, y, z, \Delta t)$ (grains/ m^2/s), during the simulation time period Δt will be calculated as

$$DS(x, y, z, \Delta t) = Q_0 \cdot Da(x, y, z) / w_s l_s / (N_p) \tag{6}$$

2.4.2 Pollen deposition on ground

If the height z of a pollen grain at the beginning of a time step is within the range $0 < z < ((-w + v_s) \cdot dt)$, the

grain will reach the ground during the time step. Let P_G be the fraction of the grains reaching the ground that is deposited [19] such that

$$P_G(w) = 2 \cdot v_s / (v_s - w); \quad w < -v_s \tag{7}$$

$$P_G(w) = 1; \quad |w| < v_s \tag{8}$$

A random number Z is chosen from a uniform distribution between 0 and 1 for each line-of-flight segment. If Z is less than P_G , then the pollen is deposited on the ground [19]. If the pollen grain is not deposited, it is reflected. The new height of the grain is

$$z = |z^{old} - 2v_s dt| \tag{9}$$

Where: z^{old} is the position of the grain at the previous time step.

2.5 Outcrossing

The grand total deposition flux GTD (grains/ m^2) at each predicted location at silk height is obtained by integrating the deposition flux density through the pollination season. The outcrossing ratio ($OutR$) (defined as the outcrossed seed number divided by the total seed number on an ear), is predicted according to the grand total deposition flux. The flowchart is shown in Figure 3. The empirical relationship between the grand total pollen deposition flux and outcrossing ratio derived from experimental data in Wang et al. [33] is used

$$OutR = GTD \times 3 \times 10^{-8} \tag{10}$$

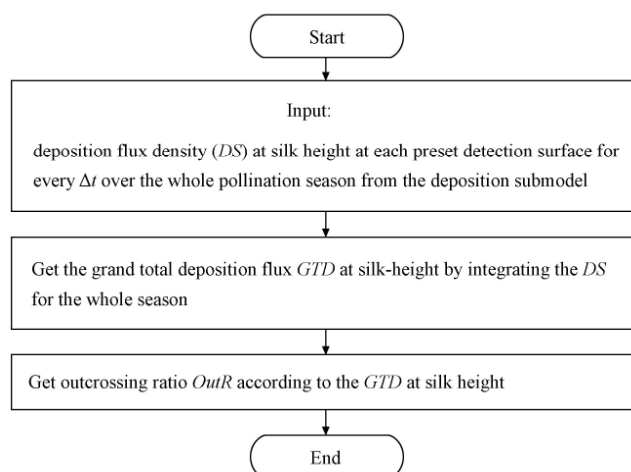


Figure 3 Flowchart of the outcrossing submodel

3 Model implementation

3.1 Simulation domain

The model of the domains includes source plant field,

buffer, and receptor plant field areas (Figure 4). The buffer area can be plants or a bare ground and can be set to different sizes for different model application purposes. Two coordinate systems are adopted. One is the cardinal coordinate system that is used in each simulation period (Δt) to simulate the dispersion and deposition of corn pollen based on the wind vector direction. The x-axis points to the mean wind vector direction in each Δt ; the y-axis points to crosswind direction; the origin is at the center of the source on the ground; and the z-axis is perpendicular to the land surface. The other coordinate system is a cylinder system that is used to define the coordinates of input and output parameters conveniently. The north direction is defined as a polar coordinate axis of $\theta = 0^\circ$. The z-axis is the same as in the cardinal coordinate system.

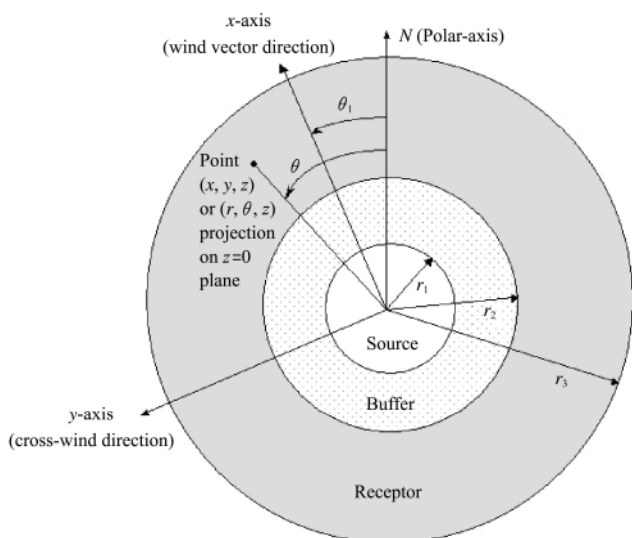


Figure 4 Model simulation domain and coordinate systems on $z = 0$ plane

The relationships between the two coordinate systems are as follows.

$$\begin{cases} x = \rho \cos(\theta - \theta_1) \\ y = \rho \sin(\theta - \theta_1) \\ z = z \end{cases} \quad (11)$$

$$\begin{cases} \rho = \sqrt{(x^2 + y^2)} \\ \theta = \begin{cases} \theta_1 + \arctan(\frac{y}{x}) & (x > 0) \\ \theta_1 + \pi + \arctan(\frac{y}{x}) & (x < 0) \end{cases} \\ z = z \end{cases} \quad (12)$$

Where: ρ is the polar radius of point (x, y, z) on the $z = 0$ plane, Q is the polar coordinate angle of point (x, y, z) , and Q_1 is the polar coordinate angle of mean wind vector. If the resultant value of $Q > 360$ in Equation (12), then the final value is set to be $(Q - 360)$.

3.2 Model inputs and outputs

Domain dimensions, plant characteristics, and weather conditions are required inputs of the model as shown in Table 2 and 3. The weather inputs, which are stored in a text file, are required at a frequency of 15 min in the pollination season. The inputted weather data is assumed to be the data at 1 m above the source canopy.

Table 3 Required weather condition inputs every 15 min

Symbol	Unit	Meaning
u^*	m/s	Friction velocity
θ_1	degree	Mean wind direction
L	m	Obukhov Length
h_m	m	Measurement height of wind data
P_r	mm	Precipitation

Every 15 min, the model outputs 3-D concentrations in and above the canopy and 2-D depositions at silk height in the receptor field from the first day of pollination season until the end of the season. This model assumes that the source and receptor start pollination season at the same time. Finally, after the pollination season, the 2-D outcrossing ratios in the receptor field were obtained. In the receptor field, a prediction column is set up every 9° angularly and at every 1.6 m radially. For concentrations, a prediction point is set up vertically at silk height (1.8 m) and at five other heights (1.6–1.8 m intervals) up to 10 m above canopy at each prediction column. For deposition flux densities, a prediction point is set up vertically at each silk height at each prediction column. For outcrossing ratios, a prediction point is set up at each prediction column.

3.3 Model implementation

The overall structure of the model was built according to the flowchart shown in Figure 1, and the plant characteristics were set based on measurements taken at the University of Connecticut Agronomy Research Farm with 8,464 Wx waxy mutant (source plant) and 8,419 W corn (receptor plant) (Garst Seeds Company, Slater, IA)

(Table 4 and section 4.1 Experiments). The plant population density was set to 71,000 plants/ha. The plant height was set to 2.9 m. Silk height was at 1.8 m. Pollen diameter was set to 82.9 μm and settling speed was set to 0.31 m/s ^[32]. In every simulation period, Δt was set to 15 min. In every Δt , the concentrations and deposition flux density at each preset prediction point were predicted. The released pollen grain number (N_p)

in each subsector at source was set to 200 (the total was 864,000 particles for all the sectors). The model runs from the first day of the pollination season to the end of the season. After the pollination season, the outcrossing ratios were calculated at the preset prediction points.

The model was programmed by C++ programming language.

Table 4 Canopy characteristics for 8464Wx and 8419W corn plants

Level	Height /m	Source plant (8,464 Wx)				Receptor plant (8,419 W)			
		$a_p/\text{m}^2 \cdot \text{m}^{-3}$	f_x	f_z	L_V/m	$a_p/\text{m}^2 \cdot \text{m}^{-3}$	f_x	f_z	L_V/m
8	2.50-2.9	0.19 (0.13)	0.40 (0.18)	0.90 (0.06)	0.021 (0.018)	0.18 (0.08)	0.58 (0.21)	0.52 (0.12)	0.009 (0.020)
7	2.15-2.50	1.13 (0.52)	0.54 (0.13)	0.80 (0.08)	0.070 (0.008)	1.15 (0.48)	0.58 (0.20)	0.69 (0.18)	0.062 (0.013)
6	1.79-2.15	1.55 (0.11)	0.52 (0.11)	0.81 (0.11)	0.076 (0.009)	2.30 (0.84)	0.52 (0.13)	0.76 (0.27)	0.072 (0.009)
5	1.43-1.79	1.85 (0.23)	0.67 (0.16)	0.67 (0.14)	0.085 (0.008)	2.40 (0.54)	0.60 (0.09)	0.65 (0.04)	0.085 (0.012)
4	1.07-1.43	1.94 (0.45)	0.65 (0.15)	0.67 (0.14)	0.082 (0.012)	2.74 (0.71)	0.75 (0.10)	0.59 (0.08)	0.062 (0.012)
3	0.72-1.07	1.51 (0.48)	0.67 (0.16)	0.63 (0.15)	0.068 (0.011)	1.87 (0.57)	0.55 (0.09)	0.69 (0.07)	0.050 (0.006)
2	0.36-0.72	0.69 (0.39)	0.56 (0.15)	0.76 (0.14)	0.045 (0.010)	1.38 (0.53)	0.68 (0.22)	0.60 (0.05)	0.051 (0.004)
1	0.00-0.36	0.24(0.23)	0.34 (0.20)	0.80 (0.14)	0.043 (0.011)	0.30 (0.23)	0.14 (0.23)	0.98 (0.22)	0.037 (0.008)

Note: Mean value is given in each cell with standard deviation in parentheses.

4 Model validation

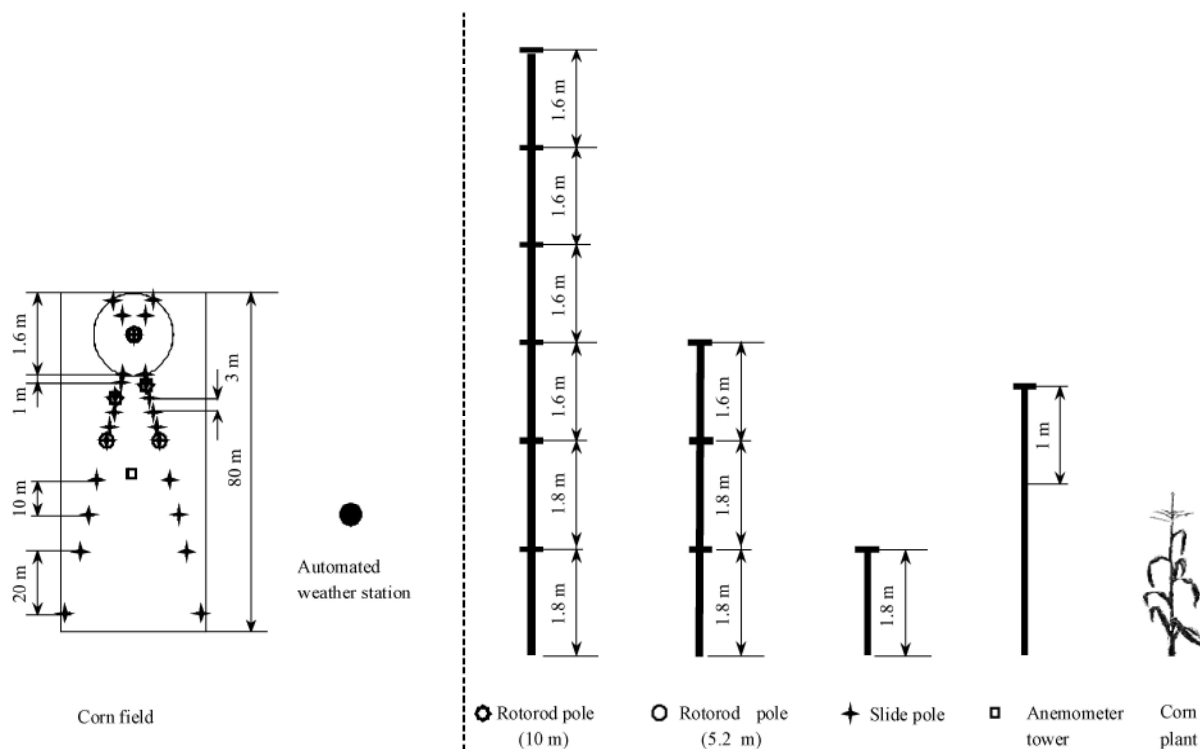
4.1 Experiments

A field experiment was conducted in the growing season of 2002 at the University of Connecticut Agronomy Research Farm to collect corn gene flow data, aiming to parameterize and validate the model. In the experiment, a circular field of source corn plants with diameter of 16 m was surrounded by a receptor field that extended 64 m from the source (Figure 5). Waxy mutant corn (8,464 Wx) with yellow kernels was planted as the source plant and regular white corn (8,419 W) as receptor plant, both with a density of 71,000 plants/ha. The field was planted in the middle of May. The average plant height was 2.9 m and the average silk height was 1.8 m for both the 8,464 Wx and 8,419 W plants. During pollination seasons, pollen concentration was measured every 1.5 or 3 hours at different heights using Rotorod samplers with retracting-type sampling heads (Model 20, Sampling Technologies, Inc., MN), and pollen deposition was measured at silk height at the same frequency by Microscope slides (2.5 by 7.5 cm) with silicon grease (Surveillance Data, Inc., Plymouth Meeting, PA), both at different distances in the source and receptor

fields. The measurements in the source field were used for the source strength calculation based on the method in Wang and Yang^[34], and the measurements in the receptor field were used for model validation. The dynamic source strength (Figure 6) was used as the model input (the data were linearly interpolated to 15 min frequency for the model implementation). Pollen release normally began in a couple of hours after sunrise, and then increased quickly with time and reached the maximum at about 10:00 am. After that, the source strength decreased. Little pollen was produced after sunset. After seeds were mature, the outcrossing ratios in the receptor field were measured. For distinguishing the pollen grains produced by the source plants from those by the receptor plants, the classical method in Brink and MacGillivray^[35] was used by applying iodine solution to stain the samples before counting under a microscope. Plants were fertilized by pollen from both 8,464 Wx and 8,419 W plants. Because the yellow endosperm allele is dominant over the white endosperm allele, kernels on the 8,419 W plants were white if the ovules were pollinated by 8,419 W and yellow if pollinated by 8,464 Wx. The seed set in the receptor field outcrossed from the source plants was therefore detected and counted by color. In

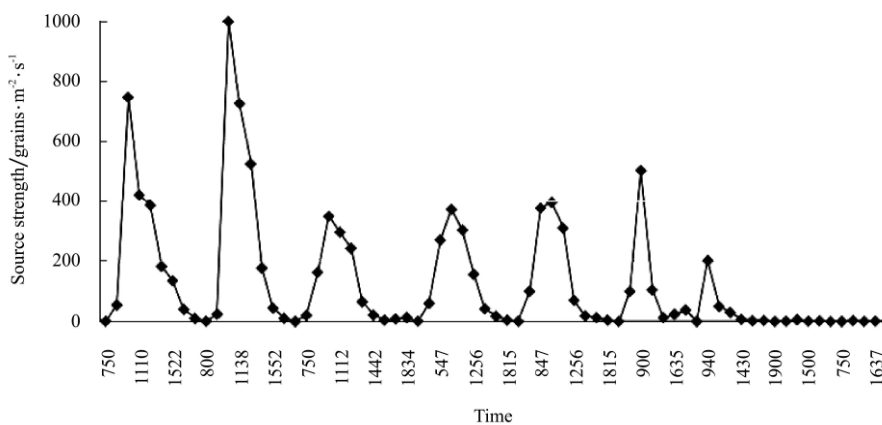
the receptor field, one ear was sampled at a point every 4 m (north-south) by 2.5 m (east-west). Outcrossing ratios were calculated for each sample from the measurements

of seed set (yellow kernel number/total kernel number on each ear).



Note: Locations of the sampling poles in the field (left) and vertical positions of the samplers on the poles (right)

Figure 5 Schematic illustration of the experimental setup



Note: The time is the local Eastern Daylight Saving Time

Figure 6 Measured pollen source strength during the pollination season.

An automated weather station was employed to measure the 15-min averages and variations of the meteorological parameters at the experimental site, including solar radiation, precipitation, air temperature, relative humidity, and wind speed and direction. In addition, two 3-D sonic anemometers (CSAT3, Campbell Scientific, Inc., Logan, UT; v-style, Applied

Technologies, Inc., Longmont, CO) were set up during the periods of pollination to measure wind profile, atmospheric stability, and turbulence. The three dimensional wind data were measured at 10 Hz and were recorded and processed to 15 min statistics (Obukhov Length, friction velocity, and wind direction) by a CR23X datalogger (Campbell Scientific, Inc., Logan, UT)

using the methods in Stull [36].

Canopy structural parameters, including leaf area density, and its vertical density distribution were measured using a leaf area meter by randomly sampling eight plants in each of the source field and the receptor field respectively (LI3100 Area Meter, Li-Cor, Inc, Lincoln, Nebraska); the results are provided in Table 4.

4.2 Validation procedure

For model validation, the 15 min data of precipitation from the weather station along with u_* , wind direction, and L from CSAT3 were used as weather inputs. In the validation process, the precipitation was always 0. The average u_* was 0.23 m/s, maximum was 0.38 m/s, and minimum was 0.17 m/s; the prevailing wind direction was 135° ; the average L was -22.8 m, maximum L was -8.7 m, and minimum L was -12,459.5 m. The plant characteristics used the data in Table 4.

Scatter plot graphs of simulated versus measured data were plotted, and linear regression between the measured and simulated data was conducted (intercept was set to zero). The linear slope of the regression with R^2 shows the accuracy of the model simulations.

Because each measurement period was 1.5 or 3 hours for concentration and deposition, the average of 15-min predicted values corresponding to each period was compared with the observation.

5 Results and discussion

5.1 Model validation

Figure 7 shows an example screen of the simulation model. This screen is a graphical concentration and deposition of the results for a 15 min simulation around noon time. The upper graph in Figure 7 shows the concentration along the mean wind direction, while the lower graph illustrates the horizontal distribution of the deposition flux at the silk height. The source field had a radius of 8 m and the receptor field had a radius of 98 m. In the lower graph, the inner circle area is the source field, and the outer one is the receptor field. The turbulence was strong ($\sigma_w=0.4$ m/s), and the concentration centerline increased with distance. However, the plume height did not increase because of corn pollen high settling speed. The deposition flux decreased exponentially with distance and most of the pollen grains were deposited close to the source field.

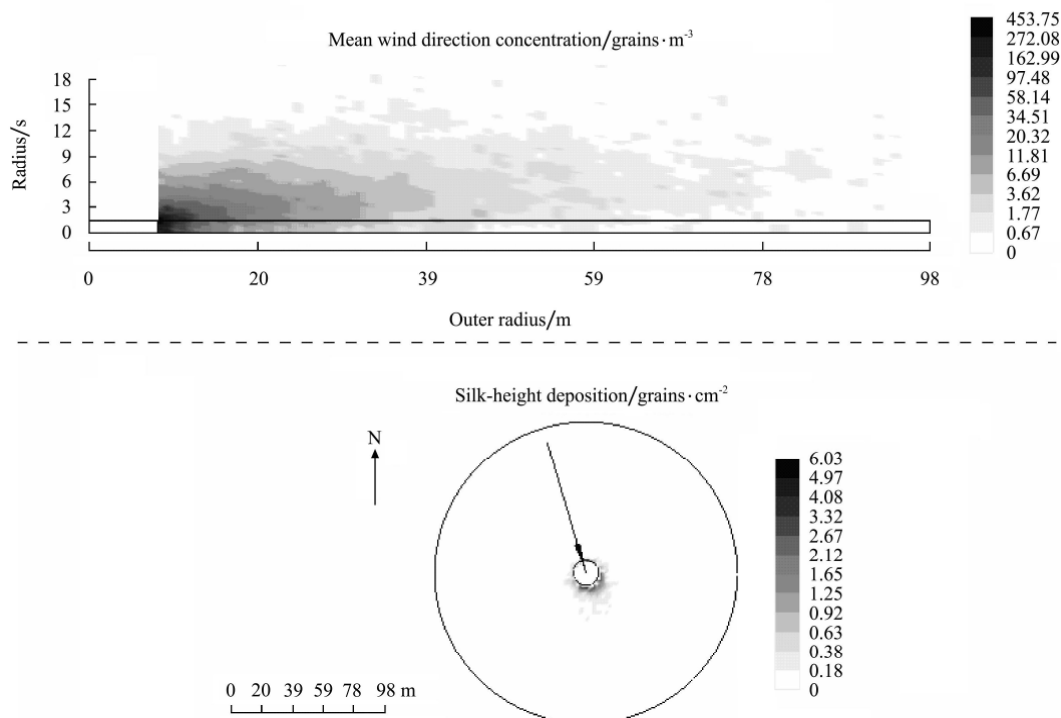


Figure 7 One sample output from the model during a noon time 15 min simulation period, when $u_* = 0.25$ m/s, wind direction = 16.5° , $L = -1$ m, and precipitation = 0 mm. The source had a radius of 8 m at the center of the simulation fields and the receptor field had an outer radius of 98 m. The arrow in the deposition graph shows the wind direction

The model was run under experimental conditions, and the results were then compared with collected data. Figures 8, 9, and 10 show the simulated versus measured concentration, deposition, and outcrossing ratio values respectively. On average, the ratio of the measured and the simulated concentration was 1.21 with $R^2 = 0.68$, the ratio of measured and simulated deposition flux density was 0.82 with $R^2 = 0.56$, and the ratio of measured and simulated outcrossing ratio was 0.85 with $R^2 = 0.60$. Therefore, the model error rate was 18% to 21% on average.

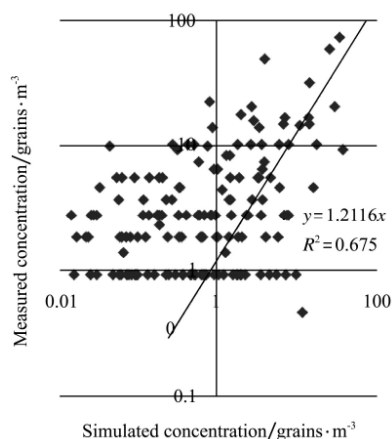


Figure 8 Measured versus simulated concentrations

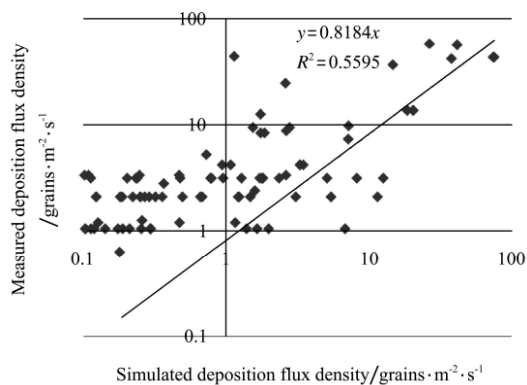


Figure 9 Measured versus simulated deposition flux density

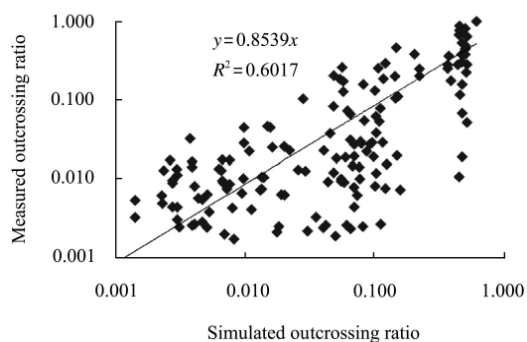


Figure 10 Simulated versus measured outcrossing ratio

This model is capable of simulating dynamic pollen release, dispersion, deposition, and final outcrossing from genetically modified corn to non-target corn plants with acceptable accuracy. This model performance was comparable to the model work of corn pollen dispersion in Klein et al.^[26] and Aylor et al.^[27]. In Klein et al.^[26], quasi-mechanistic models were used to simulate local field pollen dispersion, and the 1:1 plots for outcrossing ratios were provided for the predictions and observations (but the statistics for the prediction errors were not provided). According to their plots compared with plots in this study, the model performance in this study is comparable to their models. In Aylor et al.^[27], a Lagrangian statistical model was used to simulate pollen dispersion from near ground to 95 m height from a 23 ha corn field, and the ratio of predicted concentration was 1.4 times of the measured concentration on average. Therefore, the model accuracy in this study is comparable to the model in Aylor et al.^[27].

In the validation period, the precipitation was always 0 mm. If precipitation happens during a pollination season, the pollen source strength will be 0 during the rain and will have 0 deposition flux density in the receptor field. Precipitation may also flush out some deposited pollen grains from silks and therefore, reduce the potential outcrossing ratio. This should be investigated in the future.

5.2 Model characteristics and extensions

This model considers the dynamic pollen release, dispersion, and deposition in 15 min intervals. The flight of a pollen grain is usually simulated in time periods shorter than one second. This model more truly simulates the natural pollen transport. Because the microscale eddies have durations of 10 s to 10 min^[36], too long of a simulation step may not catch the constant variation of wind speed, direction, turbulence, and stability. For example, Tufto et al.^[25] and Klein et al.^[26] simulated pollen dispersion using whole pollination season mean wind speed and direction. Too short of a simulation step does not necessarily improve the model's performance much. In Wang et al.^[37], one-second time step had improved 1% of the accuracy of the model than a three-minute time step and 9% than a 30 min time step.

This model has the capability to simulate pollen dispersion and deposition in different canopies, which allows the model to flexibly simulate pollen dispersion in the landscape. The landscape can be bare soil, roads, or other plant species. This capability can provide a tool to choose appropriate buffer size and buffer species between source and receptor fields to prevent gene flow.

This model considers the pollen settling speed's effects on dispersion. Therefore, the model could be used for dispersion and deposition of other species' pollen, pollutant particles, and dust.

This model simulates pollen dispersion and deposition in 3-D and is therefore more realistic. The source can be points (one or a few plants) and area sources; the source can also be a volume source if the volume source is divided into small cubes. The residence time and deposition accumulator will be weighted by the small cube volume. The volume source strength will replace the area source strength in Equation (3) and (6).

The major limitation of the model is the computation time. Using a duo core computer (2.5 GHz) with 2 GB memories, the model runs over 20 h to complete for a whole pollination season. The source strength and the relationship between outcrossing ratio with grand total pollen deposition flux were measured from one experiment for one species. It may be different for different corn species and may be different under different weather conditions. This model assumes that the source and receptor start pollination season at the same time. If the two fields have different pollination seasons, it will affect the outcrossing ratio and the model needs to be modified to fit the situation. The equations for the transition wind calculations are based on Flesch and Aylor^[31]. They have not been evaluated by experimental data. Therefore, potential errors could be produced. The turbulence was produced using equations in Wilson and Shum^[30]. However, it may not capture the gust wind effects and it may produce potential model errors. Environmental condition of flat terrain where uniform wind and turbulence were assumed, was defined in this model. The wind condition could be significantly different in case of large terrain elevation changes in which Monin-Obukhov similarity theory does not work

well.

Pollen grain deposition on ground and plants or interception by plants is determined using equations in Aylor and Ferrandino^[19] and Aylor and Flesch^[20]. However, these algorithms are not evaluated by experimental data and may produce potential model errors.

6 Conclusions

The developed and validated model is capable of simulating dynamic pollen dispersion and deposition, and final outcrossing from genetically modified corn crop to non-target corn plants under different atmospheric conditions, and canopy structures with acceptable accuracy. It can be applied to aid in gene flow risk management for GM corn crops.

It can be easily adapted to predict dispersion and deposition of other species' pollen, pollutant particles, and dust under different atmospheric conditions, and canopy structures from point, area, or volume sources.

Acknowledgements

Support to the study was provided by the Storrs Agricultural Experiment Station, the University of Connecticut Research Foundation, and the University of Connecticut Environmental Research Institute. We thank the University of Connecticut farm crew (Stephen J. Olsen, Donald P. Geminani, Ronald J. Schlehofer, Gregory Tormey, and Todd Wright) for the fieldwork, and Paul Belanger from the Department of Natural Resources Management and Engineering and Yan Wu and Bernard B. Bible from Plant Science Department at University of Connecticut for their technical assistance. Especially, thank to Errol Corsan from Garst Seeds Company for his great suggestions and generous seed support, and Stephen P. Moose from Department of Crop Sciences at University of Illinois at Urbana-Champaign for his great suggestions.

[References]

- [1] Altieri M A. The environmental risks of transgenic crops: an agroecological assessment. UC Dept. Env. Sci., Pol. and Mngmnt. Berkeley, CA. 1998.

- [2] Grogan J, Long C. The problem with genetic engineering. *Organic Gardening*, 2000; (J/F): 42–47.
- [3] Bilsborrow P E, Evans E J, Bowman J, Bland B. Contamination of edible double-low oilseed rape crops via pollen transfer from high erucic cultivars. *J. Sci. Food Agric*, 1998; 76(1): 17–22.
- [4] Jones M D, Newell L C. Longevity of pollen and stigmas of grasses: buffalograss, buchhole dactyloedees (NUTT) engelm, and corn, zea mays L. *Journal of the American Society of Agronomy*, 1948; 40: 195–240.
- [5] Paterniani E, Stort A C. Effective maize pollen dispersion in the field. *Euphytica*, 1974; 23: 129–134.
- [6] Raynor G S, Hayes J V, Ogden E C. Experimental data on disersion and deposition of timothy and corn pollen from known sources. Brookhaven National Laboratory. Upton, New York. 1970a
- [7] _____. Experimental data on ragweed pollen dispersion and deposition from point and area sources. Brookhaven National Laboratory Upton, New York. 1970b
- [8] Raynor G S, Ogden E C, Hayes J V. Dispersion and deposition of corn pollen from experimental sources. *Agronomy Journal*, 1972; 64: 420–427.
- [9] Salamov A B. About isolation in corn. *Sel.i.Sem*, 3. (Russiaan translation by Michel Atanasiev in 1949). 1940.
- [10] Levin D A, Kerster H. Gene flow in seed plants. *Evolutionary Biology*, 1974; 7: 139–220.
- [11] Haldane J B S. The theory of a cline. *J of Genetics*, 1948; 48: 277–284.
- [12] Wright S. Isolation by distance. *Genetics*, 1943; 28: 114–138.
- [13] Kaimal J C, Finnigan J J. Atmospheric boundary layer flows, their structure and measurement. Oxford University Press, New York, 232 . 1994.
- [14] Fitt B D L, Gregory P H, Todd A D, McCartney H A, MacDonald O C. Spore dispersion and plant disease gradients: A comparison between two empirical models. *J. Phytopathology*, 1987; 118(3): 227–242.
- [15] Dispersal of spores and pollen from crops. *Grana*, 1994; 33(2): 76–80.
- [16] Emberlin J, Adams-Groom B, Tidmarsh J. A report on the dispersion of maize pollen. National Pollen Research Unit, University College, Worcester. <http://www.soilassociation.org/>. 1999.
- [17] Bache D H, Johnstone D R. Microclimate and spray dispersion. Ellis Horwood Limited. New York, 199222.
- [18] Aylor D E. Modeling spore dispersion in a barley crop. *Agric. Meteorol*, 1982; 26(3): 215–219.
- [19] Aylor D E, Ferrendino F J. Dispersion of spores released from an elevated line source within a wheat canopy. *Boundary-Layer Meteorol*, 1989; 46(3): 251–273.
- [20] Aylor D E, Flesch T K. Estimating spore release rates using a Lagrangian stochastic simulation model. *J. Appl. Meteorol.*, 2001; 40: 1196–1208.
- [21] Raupach M R. Dry deposition of gases and particles to vegetation. *Clean Air*, 1993; 27: 200–203.
- [22] Raupach M R, Briggs P R. Integrative modeling of transport and fate of endosulfan in the riverine environment, summary report. CSIRO Land and Water, Canberra, Australia. 1998.
- [23] Yang X, Madden L V, Brazee R D. Application of the diffusion equation for modeling splash dispersion of point-source pathogens. *New Phytol*, 1991; 295–301.
- [24] Okubo A, Levin S A. A theoretical framework for data analysis of wind dispersion of seeds and pollen. *Ecology*, 1989; 70(2): 329–338.
- [25] Tufto J, Engen S, Hindar K. Stochastic dispersal processes in plant populations. *Theor. Pop. Boil.*, 1997; (52): 16–26.
- [26] Klein E K, Lavigne C, Foueillassar X, Gouyon P H, Larédo C. Corn pollen dispersal: quasi-mechanistic models and field experiments. *Ecological Monographs*, 2003; 73(1): 131–150.
- [27] Aylor D E, Boehm M T, Shields E J. Quantifying aerial concentrations of maize pollen in the atmospheric surface layer using remote-piloted airplanes and Lagrangian stochastic modeling. *Journal of Applied Meteorology and Climatology*, 2006; 45(7): 1003–1015.
- [28] Shirolkar J S, Coimbra C F M, Queiroz McQuary M. Fundamental aspects of modeling turbulent particle dispersion in dilute flows. *Prog. Energy combust. Sci*, 1996; 22(4): 363–399.
- [29] Van den Hurk, B. J J M, Baldocchi D D. Random-walk models for simulating water vapor exchange within and above a soybean canopy. NOAA Technical Memorandum ERL ARL-185. Air Resources Laboratory. Silver Spring, Maryland. 1990.
- [30] Wilson J D, W K N Shum. A re-examination of the integrated horizontal flux method for estimating volatilization from circular plots. *Agricultural and forest Meteorology*, 1992; 57(4): 281–295.
- [31] Flesch T K, Aylor D E. A Lagrangian stochastic dispersion model for assessing pesticide spray drift in an Orchard canopy. Technical report to the U.S. Environmental Protection Agency on grant # 823627-01-1 to New Mexico State University subgrant Q00153 to the University of Connecticut, 2000.
- [32] Aylor D E. Settling speed of corn (*Zea mays*) pollen. *Journal of Aerosol Science*, 2002; 33(11): 1601–1607.
- [33] Wang J, Yang X, Li Y, Elliot P F. Pollination competition effects on gene-flow estimation: Using regular vs. male-sterile bait plants. *Agron J*, 2006; 98: 1060–1064.

- [34] Wang J, Yang X. Improved method for nondestructive measurement of dynamic pollen source strength from transgenic crops using sonic anemometer. *International Journal of Agricultural and Biological Engineering*, 2009; 2(1): 33–39.
- [35] Brink R A, MacGillivray J H. Segregation for the waxy character in maize pollen and differential development of the male gametophyte. *Am J Bot*, 1924; 11:465–469.
- [36] Stull R B. *An introduction to boundary layer meteorology*. Kluwer Academic Publishers. 2001; 181.
- [37] Wang J, Hiscox A L, Miller D R, Sammis T W. A comparison of Lagrangian model estimates to LIDAR measurements of dust plumes from field tilling. *Journal of the Air and Waste Management Association*, 2009; 59(11): 1370–1378.